

## The favoured twin: on the dynamical response of twin stars to perturbations

SHAMIM HAQUE ,<sup>1</sup> LUCIANO REZZOLLA ,<sup>2,3,4</sup> AND RITAM MALLICK ,<sup>1</sup>

<sup>1</sup>*Indian Institute of Science Education and Research Bhopal, India*

<sup>2</sup>*Institut für Theoretische Physik, Goethe Universität, Max-von-Laue-Str. 1, 60438 Frankfurt am Main, Germany*

<sup>3</sup>*School of Mathematics, Trinity College, Dublin 2, Ireland*

<sup>4</sup>*Frankfurt Institute for Advanced Studies, Ruth-Moufang-Str. 1, 60438 Frankfurt am Main, Germany*

### ABSTRACT

If a strong first-order phase transition takes place at sufficiently high rest-mass densities in the equation of state (EOS) modelling compact stars, a new branch will appear in the mass-radius sequence of stable equilibria. This branch will be populated by stars comprising a quark-matter core and a hadronic-matter envelope, i.e., hybrid stars, which represent “twin-star” solutions to equilibria having the same mass but a fully hadronic EOS. While both branches are stable to linear perturbations, it is unclear which of the twin solutions is the “favoured” one, that is, which of the two configurations is expected to be found in nature. We assess this point by performing a large campaign of general-relativistic simulations aimed at assessing the response of compact stars on the two branches to perturbations of various strength. In this way, we find that, independently of whether the stars populate the hadronic or the twin branch, their response is characterised by a critical-perturbation strength such that the star will oscillate on the original branch for subcritical perturbations and migrate to the neighbouring branch for supercritical perturbations while conserving rest-mass. Because the critical values are different for stars with the same rest-mass but sitting on either branch, it is possible to define as favoured the part of the branch that has the largest critical perturbation, thus correcting the common wisdom that stellar models on the twin branch are the favoured ones. Interestingly, we show that the binding energies on the two branches can be used to deduce without simulations which of the stellar configurations is more likely to be found in nature.

**Keywords:** Neutron stars (1108); Relativistic fluid dynamics (1389); Compact objects (288); Nuclear astrophysics (1129); Astrophysical black holes (98)

### 1. INTRODUCTION

Neutron stars (NSs) gain pressing priority when it comes to understanding the behaviour of matter at high density and low temperatures (L. Rezzolla et al. 2018; G. Baym et al. 2018; G. F. Burgio et al. 2021). These astrophysical objects are harnessed by immensely strong gravity, which allows them to compress the matter at the core well beyond the nuclear saturation density,  $\rho_{\text{sat}} \simeq 2.7 \times 10^{14} \text{ g/cm}^3$ . Quantum Chromodynamics (QCD) predicts a phase transition (PT) from hadronic matter to quark matter in such conditions, which could take place when a binary system of neutron stars collides (see, e.g., V. Paschalidis et al. 2018; E. R. Most et al. 2019; A. Bauswein et al. 2019; L. R. Weih et al. 2020; A. Prakash et al. 2021; Y.-J. Huang et al. 2022; Y. Fujimoto et al. 2023; M. Ujevic et al. 2023; S. Haque et al. 2024) or a supernova explosion takes place (see, e.g., I. Sagert et al. 2009; S. Zha et al. 2021; T. Kuroda et al. 2022; P. Jakobus

et al. 2022). This is a decades-old hypothesis that is yet to meet its complete theoretical understanding with complementing experimental (and observational) evidence.

The equation of state (EOS) of the cold neutron-rich matter is sufficiently comprehended and mainly constrained by Chiral Effective Field Theory (see, e.g., D. Lonardoni et al. 2020; C. Drischler et al. 2021). Relativistic heavy-ion collider experiments (J. Adams et al. 2005; I. Arsene et al. 2005; B. B. Back et al. 2005; K. Adcox et al. 2005) and their theoretical description (see, e.g., S. Borsányi et al. 2014; K. Nagata 2022; E. R. Most et al. 2023) efficiently probe the matter at high temperatures and low densities, and perturbative QCD calculations (S. Mogliacci et al. 2013; A. Kurkela & A. Vuorinen 2016; M. Alford & A. Sedrakian 2017; N. Haque & M. Strickland 2021; J.-E. Christian & J. Schaffner-Bielich 2022; T. Gorda et al. 2023) give reliable results only at asymptotically high densities. Hence, the NS cores, either when isolated or in binary systems, have become the promising candidates to probe the hadron-to-quark PT.

The onset of hadron-to-quark PT and the nature of this phenomenon are not known a priori (M. Oertel et al. 2017; S. Blacker et al. 2020; T. Dore et al. 2020), which leaves a plethora of possible hybrid EOSs that dictates the expression of PT inside the NS core (E. Annala et al. 2020; A. Verma et al. 2025). Under these assumptions, alternatives exist to the traditional NSs that are described by purely hadronic EOSs. In particular, it is in principle possible to consider the existence of “hybrid stars”, that is, compact stars comprising a quark-matter core and an hadronic-matter envelope.

In literature, PT has mainly been modelled as a transition using density discontinuity at a constant pressure (Maxwell construction) or a mixed-phase where hadrons and quarks co-exist (Gibbs construction) (N. K. Glendenning 2001). Importantly, the presence of a PT allows for the existence of a new branch in the mass-radius sequence of stable equilibria corresponding to hybrid stars. Because two equilibria are then possible for the same mass, the hybrid-stars are also called “twin stars” and the corresponding branch is referred to as the “twin branch” (TB), to distinguish it from the purely hadronic branch (HB) (see, e.g., M. G. Alford et al. 2013; J.-E. Christian et al. 2018; G. Montaña et al. 2019).

The bulk of work produced over the last decade on twin stars is vast and it is difficult to summarise it properly (the vast number of directions pursued in the study of twin stars has been recently reviewed by S. Haque et al. (2026) and references [90, 105-157] therein are particularly relevant for our results). Despite this rich literature, the rather fundamental issue of the “degeneracy of states” in twin stars has not been address yet. Stated differently, given the possible existence of two equilibria for the same gravitational mass, *which of these two equilibria is the favoured one?* Since equilibrium models are unable to break this degeneracy, we here address, this simple and yet challenging question by studying for the first time the response of twin and hadronic stars to nonlinear perturbations. Using general-relativistic hydrodynamical simulations we establish under what conditions a star on one of the two branches will “migrate” to the neighbouring branch to seek a new and favoured equilibrium. Because these migrations are not symmetric but reflect the different binding energies of the equilibria on the two branches, we provide a simple and intuitive criterion to determine which of the two solutions is the favoured one. More in general, this study improves the long-standing question on the nonlinear stability of equal-mass hydrostatic solutions of compact stars in general relativity.

## 2. METHODS

### 2.1. Equation of state

A strong PT in EOS is identified by a region with vanishing speed of sound, formed due to a jump in the energy density (or rest-mass density) keeping the transition pres-

$i$	1	2	3	4	5	6
$\log k_i$	-4.245	-21.197	-35.544	10.108	-64.283	-101.225
$\Gamma_i$	1.139	2.354	3.346	0.258	5.188	7.610
$\log \rho_i$	13.943	14.471	14.783	15.089	15.250	-

**Table 1.** Properties of the polytropic segments for the EOS used in this work in terms of the polytropic constants  $k_i$ , adiabatic indices  $\Gamma_i$ , and of the junction rest-mass densities  $\rho_i$  in CGS units.

sure constant (N. K. Glendenning 2001). This region defines a Maxwell-type first-order PT separating lower densities and higher densities given by hadronic-matter and quark-matter EOSs, respectively. When performing simulations in general-relativistic hydrodynamics, however, a vanishingly small the speed of sound in the PT region needs special care to avoid artefact in the numerical evolutions (J. A. Font et al. 2002; H. Dimmelmeier et al. 2009; M. Hanuske et al. 2018; P. L. Espino & V. Paschalidis 2022; X.-R. Huang et al. 2025). A simple solution to this problem consists in constructing the EOS such that the pressure is not exactly constant in the PT region and hence the speed of sound is very small but nonzero.

As a generic representative of an EOS leading to a twin-star configuration, we here consider the piecewise polytropic prescription (see, e.g., L. Rezzolla & O. Zanotti 2013) adopted in Table 1 of M. Naseri et al. (2024) where additional information can be found. This study used the EOS for general-relativistic hydrodynamic simulations of isolated hybrid stars, guaranteeing that the initial value problem remains well-posed when the PT region is included in the stellar profile. The six segments of the piecewise polytropic prescription employed here are listed in Tab. 1, where the crust is described by the polytropes  $i = 1, 2$ , the hadronic part by the polytropes  $i = 3$ , the PT region by  $i = 4$ , and, finally, the quark region is described by the polytropes  $i = 5, 6$  (note that because of our simplified treatment of the crust, we use here only six of the eight segments presented by M. Naseri et al. (2024)).

The sequences of stellar equilibrium models for the EOS considered is reported in Fig. 1 in terms of the gravitational mass  $M$  and radius  $R$ . The figure reports with a horizontal blue-shaded area the “twin region”, that is, the region in the mass-radius diagrams where the hadronic branch (HB) and the twin branch (TB) coexist in terms of rest-masses. Within the twin region, it is possible to use the turning-point criterion  $dM/d\rho_c > 0$ , where  $\rho_c$  is the central rest-mass density of the star to distinguish stable stellar models (solid lines) from the unstable ones (dashed lines); (see K. Takami et al. 2011, for a discussion of the validity of this criterion for rotating and nonrotating stars). We should note that a very similar picture would be obtained if the gravitational mass  $M$  in Fig. 1 were to be replaced by the rest-mass  $M_b$ . This is because for these

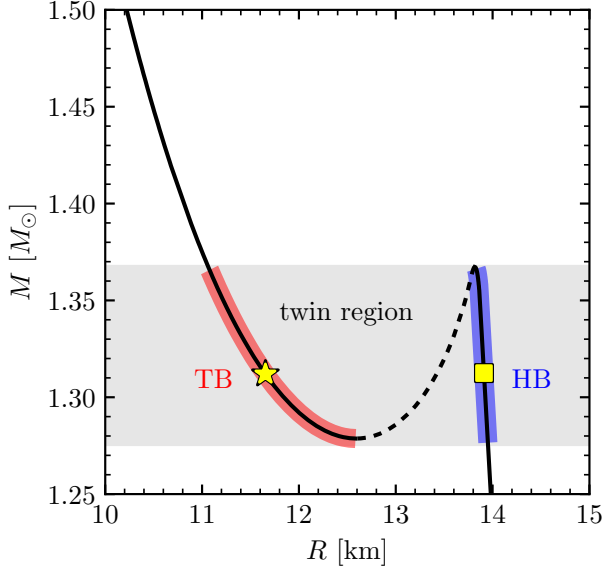


**Figure 1.** Representative example of a mass-radius sequence for an EOS leading to the coexistence of a hadronic branch (HB) and of a twin branch (TB). Solid and dashed lines are used to indicate branches that are stable or unstable to linear perturbations, respectively. Shown with a shaded area is the range in gravitational masses where the twin solutions exist, i.e., the twin region. The yellow star on TB and the yellow box on HB indicate the models TB.1.4 and HB.1.4 which are selected to discuss the migration process in Sec. 3.2. The properties of these configurations are listed in Tab. 2.

low-mass stars the two masses scale essentially linearly (see, e.g., Fig. 3 (left) of I. Garibay et al. 2026).

In both branches, we mark two stellar models having the same rest-mass  $M_b = 1.4000 M_\odot$  (yellow star for the TB and yellow box for the HB), which will be used to explain the migration process. The properties of these stellar models are listed in Tab. 2, where they are referred to as TB.1.4 and HB.1.4, respectively. Note that despite having the same rest-mass and essentially the same gravitational mass<sup>5</sup>, the two configurations have radii that differ by  $\gtrsim 2$  km, making TB.1.4 significantly more compact than HB.1.4. As a result, the matter in the core of TB.1.4 is compressed enough such that the central core is described by a quark-matter EOS, while HB.1.4 is purely made of hadronic matter.

## 2.2. Numerical Setup

To study the nonlinear response to perturbations of twin and hadronic stars we have employed the open-source code GR1D<sup>6</sup> (E. O’Connor & C. D. Ott 2010), which solves the spherically symmetric general-relativistic hydrodynamic equations with a finite-volume scheme, piecewise-parabolic

<sup>5</sup> We recall that a quasi-universal relation can be used to relate  $M$  and  $M_b$  analytically (F. X. Timmes et al. 1996; I. Garibay et al. 2026).

<sup>6</sup> <https://github.com/evanoconnor/GR1D>

Model	$\rho_c/\rho_{\text{sat}}$	$M [M_\odot]$	$M_b [M_\odot]$	$R [\text{km}]$
TB.1.4	5.7342	1.3119	1.4000	11.6540
HB.1.4	2.2227	1.3124	1.4000	13.9110

**Table 2.** Properties of the representative stellar models indicated in Fig. 1 with a yellow star and the yellow box. These models are selected to explore the migration process in Sec. 3.2.

reconstruction and an HLLE Riemann solver (see, e.g., L. Rezzolla & O. Zanotti 2013). The initial data is obtained via the solution of the Tolman-Oppenheimer-Volkoff (TOV) equations. A uniform one-dimensional (1D) spatial grid is used with a resolution of 100 m and the outer boundary is extended to 200 km (additional resolutions at 50 m and 25 m have been studied to explore the converge of the solutions). The temporal evolution uses the method-of-lines to a second-order Runge-Kutta scheme with a Courant-Friedrichs-Lowy (CFL) condition set to 1/2. An atmosphere with a constant density of 1 g/cm<sup>3</sup> is set outside the stellar profile. We finally note that because of the computational costs associated with our large campaign of simulations, we have here resorted to the use of 1D simulations. However, some of the simulations have also been performed with the publicly available and fully three-dimensional (3D) general-relativistic hydrodynamic code WhiskyTHC (D. Radice et al. 2014) obtaining very similar results.

## 3. RESULTS

### 3.1. Initial Perturbations

As first shown by J. A. Font et al. (2002) using three-dimensional general-relativistic simulations, a stellar model that is in an unstable equilibrium can “migrate” to an equilibrium configuration as a response to perturbations and while conserving rest-mass. A similar process is expected to take place also in the case of stars on the TB and HB, with the important difference that, in this case, both of the stellar models are expected to be in a stable equilibrium. Despite stability with respect to *linear* perturbations, one of the two stable configuration may be “favoured” over the other, so that, when subject to *nonlinear* perturbations, a star on the TB or HB will either oscillate in its original branch or migrate to the neighbouring one. This migration can either take place via an expansion to larger radii, i.e., a TB → HB transition, or via a compression to more compact configurations, i.e., a HB → TB transition.

To trigger such a transition, we introduce a perturbation that could reflect a plausible astrophysical scenario, such as a stellar spin-down, or the accretion of matter on the stellar surface, we introduce a constant inward radial velocity of different strength on the initial static stellar models, i.e.,

$$v^r/c = 0 \quad \rightarrow \quad v^r/c = -\lambda_{\text{H,T}}, \quad (1)$$

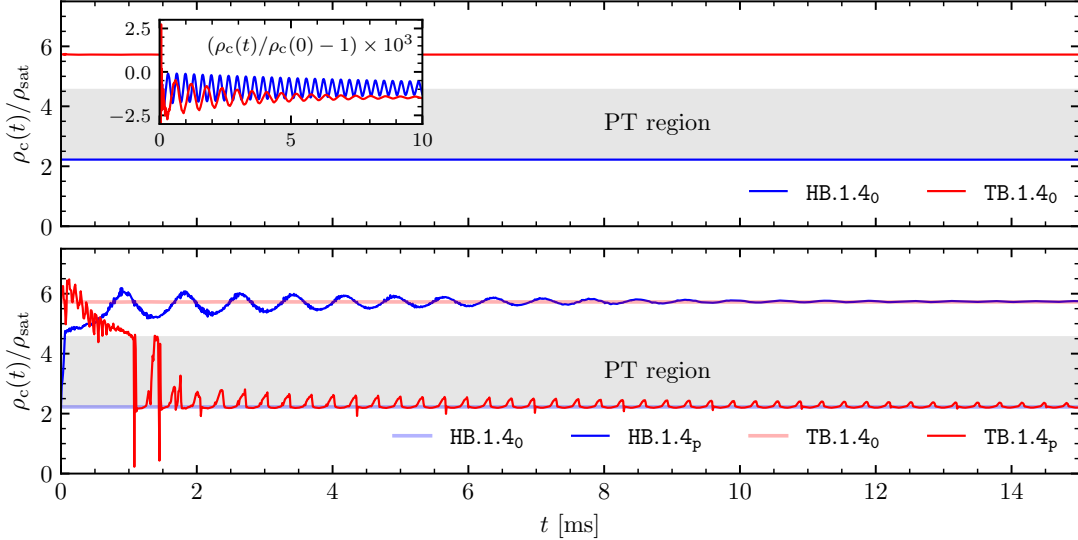


**Figure 2.** *Top panel:* Evolution of the central rest-mass density  $\rho_c$  normalised to the nuclear-saturation density for the representative stellar configurations TB.1.4 and HB.1.4 that are shown with yellow symbols in Fig. 1 (see also Tab. 2). Because no perturbations are introduced in this case, the inset is needed to show the minute relative oscillations and their decay with time. The shaded area reports the range of rest-mass densities across which the PT takes place. Clearly, both TB.1.4 and HB.1.4 are stable to linear perturbations. *Bottom panel:* the same as in the top but when the stars experience critical perturbations. In both cases, the stars migrate to the neighbouring branch of static solutions.

where  $\lambda_{H,T} > 0$  measures the strength of the perturbation and the index H, T indicates whether the star is initially on the HB or on the TB. Because extremely large perturbations would be incompatible with the assumption of adiabatic evolutions, we limit the strength of the initial perturbation to  $\lambda_{H,T} < 0.1 c$ ; as we discuss below, such strength is sufficient to obtain all the relevant results.

Ideally, it would be preferable to introduce perturbations with suitable perturbative eigenfunctions in all hydrodynamical quantities. In practice, and as done customarily in this type of studies (see, e.g., H. Dimmelmeier et al. 2009; D. Radice et al. 2014; S. Shashank et al. 2023; T. Pierre Jacques et al. 2025), the solution of the full set of hydrodynamical equations is such that over a couple of dynamical timescales the star recovers the correct behaviour with the eigenfunctions in the hydrodynamical variables matching well the perturbative ones.

We should also note that, as mentioned above, the EOS employed here is meant to describe zero-temperature matter in beta equilibrium. To reflect a purely adiabatic treatment of the perturbations – and hence not to contaminate the dynamics with the inclusion of dissipative heating – no additional thermal contribution is added to the pressure during the evolution. This is a very good approximation given the modest velocity perturbations introduced and the fact that they do not lead to shocks.

### 3.2. Migration dynamics

The top panel of Fig. 2 reports the evolutions of our two reference stellar configurations without external perturba-

tions, which we will refer to as HB.1.4<sub>0</sub> (black solid line) and TB.1.4<sub>0</sub> (red solid line), respectively. More specifically, shown is the central rest-mass density  $\rho_c$  when normalised to  $\rho_{\text{sat}}$ . The two lines appear as perfectly horizontal here but this is just the consequence of the scale used and the minuteness of the perturbations that are triggered uniquely by the truncation error in the discretisation of the equilibrium models. Shown however in the inset is the central rest-mass density normalised to its initial value  $\rho_c(t=0)$ ; the scale is sufficiently magnified so as to appreciate that there indeed are oscillations and that these are of  $\simeq 0.1\%$ . It is then clear that in both cases  $\rho_c$  oscillates around an equilibrium value<sup>7</sup> and that the oscillations eventually damp out at later time steps as a result of the small but nonzero to numerical bulk viscosity (P. Cerdá-Durán 2010; M. Chabanov & L. Rezzolla 2025). Also clear is that the oscillations have different frequencies as expected for stars of different compactnesses, with HB.1.4<sub>0</sub> having an  $f$ -mode frequency that is  $\sim 1.74$  times larger than that of TB.1.4<sub>0</sub>. Overall, the results of the top panel of Fig. 2 indicate that both HB.1.4 and TB.1.4 are stable with respect to linear perturbations.

By performing a very large number of simulations in which the strength of the initial perturbation, i.e.,  $\lambda_{H,T}$ , has revealed that a threshold critical perturbation determines whether a perturbed star (either on the HB or the TB) will migrate

<sup>7</sup> We note that the equilibrium is towards slightly larger central rest-mass density values because the numerical import naturally introduces a difference in the equilibrium model (see L. Baiotti et al. 2005, for a first discussion of this issue).

to the neighbouring branch. In other words, referring to Eq. (1) there appears a critical value  $\lambda_{H,\text{crit}}$  such that a perturbed star initially on the HB remain on the HB for perturbations  $\lambda_H < \lambda_{H,\text{crit}}$  while it will migrate to the TB for  $\lambda_H \geq \lambda_{H,\text{crit}}$ . Similar considerations apply to stars initially on the TB, such that the star will remain on the TB for perturbations  $\lambda_T < \lambda_{T,\text{crit}}$  while it will migrate to the HB for  $\lambda_T \geq \lambda_{T,\text{crit}}$ .

To illustrate the dynamics of the migration, the bottom panel of Fig. 2 reports the evolution of the same models discussed in the top panel but when a critical perturbation is used for the migration on either side, i.e.,  $\lambda_H = \lambda_{H,\text{crit}} = 0.021 c$  and  $\lambda_T = \lambda_{T,\text{crit}} = 0.040 c$ . We refer to these models as HB.1.4<sub>p</sub> and TB.1.4<sub>p</sub>, respectively and report as a reference also in the bottom panel the evolution of the models HB.1.4<sub>0</sub> and TB.1.4<sub>0</sub>.

For the stellar model HB.1.4<sub>p</sub>, the initial infall velocity perturbation induces a mini-collapse, with a rapid contraction of the star and an increase in the central rest-mass density  $\rho_c$  over a timescale of  $\sim 0.1$  ms. Since  $\rho_c$  of HB.1.4<sub>p</sub> (black solid line) is located close to the PT region, the perturbation is strong enough to trigger a PT inside the core and hence generate quark matter in the star. As a result,  $\rho_c$  continues to grow until the matter becomes sufficiently stiff enough to exert an outward balancing pressure to halt the collapse around  $t \sim 1$  ms. This results in  $\rho_c$  starting to oscillate around an equilibrium value. As the evolution proceeds (we have carried out the simulations up to  $t \simeq 50$  ms), the oscillations tend to decay and  $\rho_c$  settles around the value corresponding to model TB.1.4<sub>0</sub> with a precision of 0.36%. After about  $\sim 20$  ms, the system has reached its new equilibrium and a successful HB  $\rightarrow$  TB migration has taken place.

A complementary dynamics is shown by the stellar model TB.1.4<sub>p</sub>, where the initial radial kick similarly induces an increase in  $\rho_c$ , which however excites the high-frequency oscillation modes. In this case, however, the collapse is immediately halted by the stiff quark-matter EOS, thus resulting in a rapid bounce and outward expansion of the whole star. The resulting decompression allows for the central rest-mass density to enter at  $t \sim 1$  ms the high-density edge of the PT region in the EOS (the EOS at the PT region can be thought to be extremely soft) and hence undergo a very rapid expansion. As a result of the reverse PT, the star is purely hadronic and the central density oscillates around the low-density edge of the PT region while attaining a new equilibrium, which corresponds to that of HB.1.4<sub>0</sub> with a precision of 0.18%. Also in this case, the oscillations are gradually damped and after about  $\sim 20$  ms, the system has reached its new equilibrium and a successful TB  $\rightarrow$  HB migration has taken place.

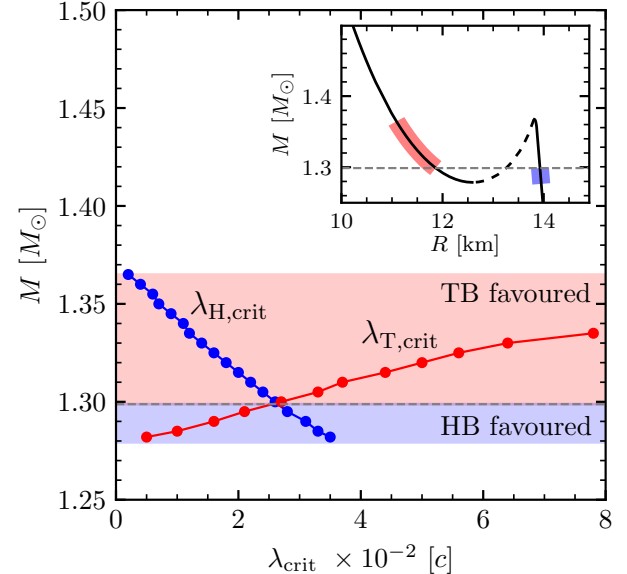


**Figure 3.** Numerical values of the critical perturbation velocities  $\lambda_{T,\text{crit}}$  for models on the TB (filled blue circles) and the corresponding values  $\lambda_{H,\text{crit}}$  for models on the HB (filled red circles) for the range of masses in the twin region. The different colours in the two shaded regions show which of the two branches is favoured when comparing  $\lambda_{T,\text{crit}}$  and  $\lambda_{H,\text{crit}}$ ; shown with a horizontal dashed line is the value of the neutral-favouritism mass  $M_{\text{neut}} = 1.2988 M_\odot$ , where the two branches are equally favoured. Shown in the inset is a representation of the favourite branches in an  $(M, R)$  diagram.

### 3.3. Critical perturbations and favoured twin solutions

The simulations described above for the HB.1.4 and TB.1.4 models have been repeated for a large number of stellar models with different baryonic (and gravitational) masses. The dynamics is then essentially the same but with the important difference that the critical perturbation velocity is a function of the mass, i.e.,  $\lambda_{T,\text{crit}} = \lambda_{T,\text{crit}}(M)$  and  $\lambda_{H,\text{crit}} = \lambda_{H,\text{crit}}(M)$ . Figure 3 highlights this mass dependence by reporting the critical values for both branches as a function of the gravitational mass. Interestingly, the behaviour of the two critical perturbations with  $M$  is very different, so that, in general,  $\lambda_{T,\text{crit}} \neq \lambda_{H,\text{crit}}$ .

These results are very revealing as they show that although migrations in both directions are possible, i.e.,  $\text{HB} \rightleftharpoons \text{TB}$ , they are not equally likely. On the contrary, a star on a given branch will prefer to stay on that branch unless it is subject to a very large (and possibly unrealistic) perturbation is experienced. In turn, this allows us to introduce criterion discriminating which of the two twins is the “favoured” one. More specifically, we conclude that

$$\text{TB is favoured if } \lambda_{T,\text{crit}}(M) < \lambda_{H,\text{crit}}(M), \quad (2)$$

$$\text{HB is favoured if } \lambda_{T,\text{crit}}(M) > \lambda_{H,\text{crit}}(M), \quad (3)$$

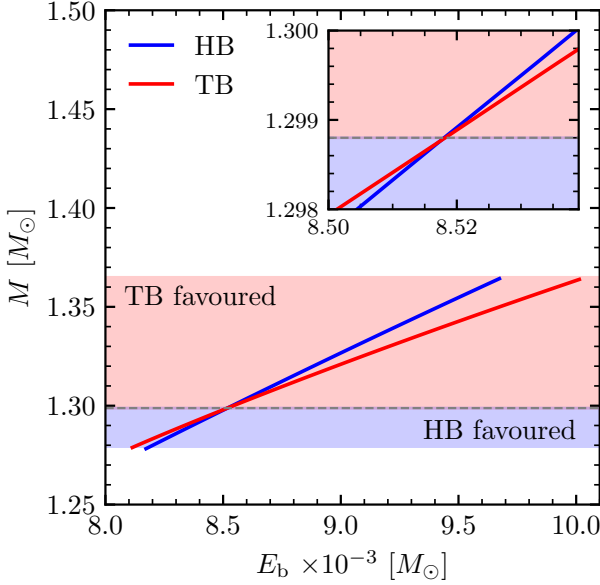


**Figure 4.** The same as in Fig. 3 but in terms of the binding energy  $E_b := M_b - M$ ; the inset shows a magnified view of the binding energies near the neutral mass  $M_{\text{neut}} = 1.2988 M_\odot$ . Clearly, the representations in terms of  $E_b$  and  $\lambda_{\text{crit}}$  are very similar, so that the binding energies can be used to deduce the favoured twin without resorting to numerical simulations.

with a “neutral favouritism” condition (analogous to a “neutral stability” condition) when

$$\lambda_{T,\text{crit}}(M = M_{\text{neut}}) = \lambda_{H,\text{crit}}(M = M_{\text{neut}}). \quad (4)$$

For the specific EOS considered here, this latter condition is met for a neutral mass  $M_{\text{neut}} = 1.2988 M_\odot$  and is marked by an horizontal dashed line in Fig. 3. Overall, the response of twin and hadronic stars to perturbations nicely summarised in Fig. 3 points out what is possibly the most important result of this paper, namely, that the common wisdom that stellar models on the TB are those more likely to be found in nature is actually incorrect. On the contrary, the response to perturbations analysed here clearly shows that low-mass hadronic stars are favoured over the corresponding twin solution. Furthermore, as we will discuss in Sec. 3.4, the actual existence of stars on the TB may be highly unlikely if the PT is very large.

The existence of favoured and neutral stellar configurations can be intuitively understood if one bears in mind that stable equilibrium stellar models can be associated in a classical sense to local ground states of the Einstein equations, therefore as sitting at the bottom of the local minimum of an effective potential that depends on the perturbation strength. When subject to small (linear) perturbations, their energy will be varied by the introduction of the energy in the perturbation, which will induce oscillations around the ground states. So long as the energy perturbation is smaller than the

potential barrier, the configuration will remain in the same local (and false) minimum or, equivalently, a star in a favoured branch will remain in such a branch. However, if the energy in the perturbation is sufficiently large to overcome the potential barrier, a second local minimum will become the true minimum and the star will move to it. This is what happens when a star on a given branch migrates to the neighbouring one for  $\lambda_{H,T} \geq (\lambda_{H,T})_{\text{crit}}$ . Clearly, if the two minima are identical, both branches are equally favoured, hence the existence of a neutral mass where this happens. The concept of neutral mass the distinction between the favoured branches in the  $(M, R)$  plane is summarised in the inset of Fig. 3.

If the existence of a neutral mass  $M_{\text{neut}}$  is rather natural, a final point to clarify is what determines it. This can be easily addressed by comparing the gravitational binding energies  $E_b := M_b - M > 0$  of the stellar models on the two branches. This is shown in Fig. 4, which reports the binding energy for stars on the HB (blue solid line) and on the TB (red solid line). Although these energies are very similar, they are not identical and, interestingly, they coincide at  $M = M_{\text{neut}}$ . The mapping between  $\lambda_{\text{crit}}$  and  $E_b$  is true with a precision of 0.1%. This result clearly illustrates that, for any gravitational mass, the favoured stars are those with the largest binding energy as they are sitting in the true equilibrium state. Furthermore, it shows that the potential-barrier differences – which are effectively mapped to the difference  $|\lambda_{H,\text{crit}} - \lambda_{T,\text{crit}}|$  – are smaller for  $M < M_{\text{neut}}$ , which also explains why in Fig. 3 the difference in critical migration values, i.e.,  $|\lambda_{H,\text{crit}} - \lambda_{T,\text{crit}}|$ , is smaller for masses below the neutral one.

#### 3.4. Other classes of twin stars

The picture summarised above refers to twin stars that are classified to belong to category III (J.-E. Christian et al. 2018; G. Montaña et al. 2019), that is, stars for which the maximum mass of the HB is smaller than the maximum mass of the TB, i.e.,  $M_{\text{TOV,HB}} < M_{\text{TOV,TB}}$ ; for obvious reasons, a very similar response is expected also for categories I, and IV of the same classification. However, there is a fourth category, for which the opposite is true, that is,  $M_{\text{TOV,TB}} \leq M_{\text{TOV,HB}}$ , and this is referred to as category II (J.-E. Christian et al. 2018; G. Montaña et al. 2019). These configurations are shown in the left panel of Fig. 5, which reports three different EOSs with  $M_{\text{TOV,TB}} = M_{\text{TOV,HB}} = 2.010 M_\odot$ , but also  $M_{\text{TOV,TB}} = 1.754 M_\odot$  and  $1.389 M_\odot$ .

The response of these compact-star configurations to perturbations can be easily deduced without performing numerical simulations (which we have however performed), by simply looking at the binding energies of the different stellar models. These are reported in the right panel of Fig. 5 and it then appears clear that while the first two EOSs from the top lead to binding-energy curves that cross at some spe-

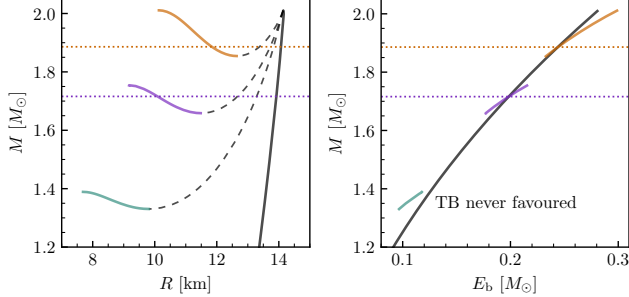


**Figure 5.** *Left panel:* the same as in Fig. 1 but for three EOSs that lead to twin stars of category II. The stable HB is marked with a black solid line, while the stable TBs are marked with solid lines of different colours; dashed and dotted lines mark the (linearly) unstable branches and the neutral masses  $M_{\text{neut}}$ , respectively. *Right panel:* the same as in Fig. 4 but for the three EOSs on the left panel; also here, the coloured dotted lines mark the neutral masses. Note that no neutral mass exists for the EOS with the smallest maximum mass on the TB; hence, no stellar model on the TB is favoured for this EOS.

specific value of the neutral mass (i.e.,  $M_{\text{neut}} = 1.886 M_{\odot}$  and  $1.716 M_{\odot}$ ) the third EOS leads to sequences of stellar models whose binding energies never intersect. As a result, for this EOS, no neutral mass exists and only one branch will be favoured. Indeed, this is exactly what we find via numerical simulations, which reveal that  $\lambda_{T,\text{crit}} < \lambda_{H,\text{crit}}$  for all stars on the TB with  $M \lesssim 1.355 M_{\odot}$ . At the same time, the response to perturbations of stars on the TB having mass  $M \gtrsim 1.355 M_{\odot}$  is such that they will not migrate towards the HB, but rather collapse to black holes as a result of the radial-velocity perturbation. Unsurprisingly, smaller and smaller perturbations are needed as the mass of the perturbed star approaches  $M_{\text{TOV,TB}}$ . Overall, this phenomenology reveals a very intriguing new behaviour of very compact twin-star configurations, where a new criticality in the behaviour – i.e., the criticality to collapse to black holes – appears in addition to criticality to migration. We will explore this in more detail in a forthcoming paper.

#### 4. CONCLUSION

Twin stars are the manifestation of the occurrence of a first-order PT and have been the subject of numerous investigations over the last decade. While it is simple to distinguish which of the compact-star solutions resides on a branch that is stable to linear perturbations, much more difficult is to predict which of the twin solutions is the “favoured” one, that is, which of the two possible stable configurations is expected to be found in nature. We have addressed this simple but fundamental question by studying via fully general-relativistic simulations the response of stars on the TB and HB to non-linear perturbations triggered by an initial inward radial velocity of various strength.

In this way, we have found that the response of all stellar models, independently of whether they sit on the hadronic or twin branch, is characterised by a critical-perturbation strength. For subcritical perturbations the star will oscillate on the original branch with damped oscillations, while for supercritical perturbations it will migrate to the neighbouring branch, where it will eventually settle to the corresponding equilibrium having the same rest-mass. More importantly, the critical values on the hadronic and twin branches depend on the mass of the star but are different for the same mass, so that it is possible to define as “favoured” the part of the branch which has the largest critical perturbation, as one expects that this represents the true ground system of the space of configurations.

Interestingly, we have also found that the differences in critical perturbations can be mapped into differences in the binding energies of the stellar models on the two branches. As a result, the favoured star is simply that with the largest binding energy and a (neutral) mass appears where the favouritism is neutral and both configurations are equally favoured. Hence, a simple investigation of the binding energies on the two branches will reveal which of the stellar configurations is more likely to be found in nature. Finally, while our results have been applied to an EOS leading to a specific class of twin stars, i.e., categories I, III, and IV of the classification in G. Monta  a et al. (2019), we have shown, both with simulations and with the binding energies, that the conclusions drawn above hold true also in other classes of twin stars.

Overall, these results demonstrate that the common wisdom for which the stellar models on the twin branch are the one expected to be revealed by observations is, at least in part, incorrect. Indeed, it is reasonable to expect stars that should populate the low-mass part of the TB are not found in nature, and that the corresponding models should exist as stable hadronic stars or black holes.

Finally, while this study significantly improves our understanding of the long-standing issue of the existence of twin-star solutions, it can be extended in a number of ways. First, by a more extensive validation of the location of the critical perturbations via 3D simulations and the inclusion of non-spherical perturbations. Second, by the inclusion of a broader set of EOSs that may reveal quasi-universal properties in the neutral-favouritism mass  $M_{\text{neut}}$ , which, in turn, could be used to set tighter constraints on the existence of twin stars. Third, by extending the set of initial configurations considered to include configurations that are rotating and magnetised. We plan to explore these aspects in future work.

## ACKNOWLEDGMENTS

It is a pleasure to thank Mark Alford, M. Hanauske, J. Schaffner-Bielich, A. Sedrakian, S. Chatterjee, T. P. Jacques, and Samuel Tootle for helpful discussions and useful feedback. SH and RM acknowledge the SERB grant: CRG/2022/000663. Partial funding comes from the ERC Advanced Grant ‘‘JETSET: Launching, propagation and emission of relativistic jets from binary mergers and across mass

scales’’ (Grant No. 884631). LR acknowledges the Walter Greiner Gesellschaft zur Förderung der physikalischen Grundlagenforschung e.V. through the Carl W. Fueck Laureatus Chair.

*Software:* GR1D (E. O’Connor & C. D. Ott 2010), NUMPY (C. R. Harris et al. 2020), MATPLOTLIB (J. D. Hunter 2007), JUPYTER (T. Kluyver et al. 2016)

## REFERENCES

Adams, J., Aggarwal, M., Ahammed, Z., et al. 2005, Nuclear Physics A, 757, 102, doi: [10.1016/j.nuclphysa.2005.03.085](https://doi.org/10.1016/j.nuclphysa.2005.03.085)

Adcox, K., Adler, S. S., Afanasiev, S., et al. 2005, Nuclear Physics A, 757, 184, doi: [10.1016/j.nuclphysa.2005.03.086](https://doi.org/10.1016/j.nuclphysa.2005.03.086)

Alford, M., & Sedrakian, A. 2017, Phys. Rev. Lett., 119, 161104, doi: [10.1103/PhysRevLett.119.161104](https://doi.org/10.1103/PhysRevLett.119.161104)

Alford, M. G., Han, S., & Prakash, M. 2013, Phys. Rev. D, 88, 083013, doi: [10.1103/PhysRevD.88.083013](https://doi.org/10.1103/PhysRevD.88.083013)

Annala, E., Gorda, T., Kurkela, A., Nättilä, J., & Vuorinen, A. 2020, Nat. Phys., 16, 907, doi: [10.1038/s41567-020-0914-9](https://doi.org/10.1038/s41567-020-0914-9)

Arsene, I., Bearden, I. G., Beavis, D., et al. 2005, Nuclear Physics A, 757, 1, doi: [10.1016/j.nuclphysa.2005.02.130](https://doi.org/10.1016/j.nuclphysa.2005.02.130)

Back, B. B., Baker, M. D., Ballintijn, M., et al. 2005, Nuclear Physics A, 757, 28, doi: [10.1016/j.nuclphysa.2005.03.084](https://doi.org/10.1016/j.nuclphysa.2005.03.084)

Baiotti, L., Hawke, I., Montero, P. J., et al. 2005, Phys. Rev. D, 71, 024035, doi: [10.1103/PhysRevD.71.024035](https://doi.org/10.1103/PhysRevD.71.024035)

Bauswein, A., Bastian, N.-U. F., Blaschke, D. B., et al. 2019, Phys. Rev. Lett., 122, 061102, doi: [10.1103/PhysRevLett.122.061102](https://doi.org/10.1103/PhysRevLett.122.061102)

Baym, G., Hatsuda, T., Kojo, T., et al. 2018, Rep. Prog. Phys., 81, 056902, doi: [10.1088/1361-6633/aaae14](https://doi.org/10.1088/1361-6633/aaae14)

Blacker, S., Bastian, N.-U. F., Bauswein, A., et al. 2020, Phys. Rev. D, 102, 123023, doi: [10.1103/PhysRevD.102.123023](https://doi.org/10.1103/PhysRevD.102.123023)

Borsányi, S., Fodor, Z., Hoelbling, C., et al. 2014, Physics Letters B, 730, 99, doi: [10.1016/j.physletb.2014.01.007](https://doi.org/10.1016/j.physletb.2014.01.007)

Burgio, G. F., Schulze, H. J., Vidaña, I., & Wei, J. B. 2021, Progress in Particle and Nuclear Physics, 120, 103879, doi: [10.1016/j.ppnp.2021.103879](https://doi.org/10.1016/j.ppnp.2021.103879)

Cerdá-Durán, P. 2010, Classical and Quantum Gravity, 27, 205012, doi: [10.1088/0264-9381/27/20/205012](https://doi.org/10.1088/0264-9381/27/20/205012)

Chabanov, M., & Rezzolla, L. 2025, PhRvD, 111, 044074, doi: [10.1103/PhysRevD.111.044074](https://doi.org/10.1103/PhysRevD.111.044074)

Christian, J.-E., & Schaffner-Bielich, J. 2022, ApJ, 935, 122, doi: [10.3847/1538-4357/ac75cf](https://doi.org/10.3847/1538-4357/ac75cf)

Christian, J.-E., Zacchi, A., & Schaffner-Bielich, J. 2018, Eur. Phys. J. A, 54, 28, doi: [10.1140/epja/i2018-12472-y](https://doi.org/10.1140/epja/i2018-12472-y)

Dimmelmeier, H., Bejger, M., Haensel, P., & Zdunik, J. L. 2009, Mon Not R Astron Soc, 396, 2269, doi: [10.1111/j.1365-2966.2009.14891.x](https://doi.org/10.1111/j.1365-2966.2009.14891.x)

Dore, T., Noronha-Hostler, J., & McLaughlin, E. 2020, Phys. Rev. D, 102, 074017, doi: [10.1103/PhysRevD.102.074017](https://doi.org/10.1103/PhysRevD.102.074017)

Drischler, C., Holt, J. W., & Wellenhofer, C. 2021, Annual Review of Nuclear and Particle Science, 71, 403, doi: [10.1146/annurev-nucl-102419-041903](https://doi.org/10.1146/annurev-nucl-102419-041903)

Espino, P. L., & Paschalidis, V. 2022, Phys. Rev. D, 105, 043014, doi: [10.1103/PhysRevD.105.043014](https://doi.org/10.1103/PhysRevD.105.043014)

Font, J. A., Goodale, T., Iyer, S., et al. 2002, Phys. Rev. D, 65, 084024, doi: [10.1103/PhysRevD.65.084024](https://doi.org/10.1103/PhysRevD.65.084024)

Fujimoto, Y., Fukushima, K., Hotokezaka, K., & Kyutoku, K. 2023, Phys. Rev. Lett., 130, 091404, doi: [10.1103/PhysRevLett.130.091404](https://doi.org/10.1103/PhysRevLett.130.091404)

Garibay, I., Ecker, C., & Rezzolla, L. 2026, arXiv e-prints, arXiv:2601.07931, doi: [10.48550/arXiv.2601.07931](https://doi.org/10.48550/arXiv.2601.07931)

Glendenning, N. K. 2001, Physics Reports, 342, 393, doi: [10.1016/S0370-1573\(00\)00080-6](https://doi.org/10.1016/S0370-1573(00)00080-6)

Gorda, T., Paatela, R., Säppi, S., & Seppänen, K. 2023, Phys. Rev. Lett., 131, 181902, doi: [10.1103/PhysRevLett.131.181902](https://doi.org/10.1103/PhysRevLett.131.181902)

Hanauske, M., Yilmaz, Zekiye Simay, Mitropoulos, Christina, Rezzolla, Luciano, & Stöcker, Horst. 2018, EPJ Web Conf., 171, 20004, doi: [10.1051/epjconf/201817120004](https://doi.org/10.1051/epjconf/201817120004)

Haque, N., & Strickland, M. 2021, Phys. Rev. C, 103, L031901, doi: [10.1103/PhysRevC.103.L031901](https://doi.org/10.1103/PhysRevC.103.L031901)

Haque, S., Mallick, R., & Thakur, S. K. 2024, Mon Not R Astron Soc, 527, 11575, doi: [10.1093/mnras/stad3839](https://doi.org/10.1093/mnras/stad3839)

Haque, S., Shinde, A., Saha, A. K., Malik, T., & Mallick, R. 2026, Investigating Twin Star Equation of States in Light of Recent Astrophysical Observations, arXiv, doi: [10.48550/arXiv.2601.16674](https://doi.org/10.48550/arXiv.2601.16674)

Harris, C. R., et al. 2020, Nature, 585, 357, doi: [10.1038/s41586-020-2649-2](https://doi.org/10.1038/s41586-020-2649-2)

Huang, X.-R., Zha, S., Chu, M.-c., O’Connor, E. P., & Chen, L.-W. 2025, ApJ, 979, 151, doi: [10.3847/1538-4357/ada146](https://doi.org/10.3847/1538-4357/ada146)

Huang, Y.-J., Baiotti, L., Kojo, T., et al. 2022, Phys. Rev. Lett., 129, 181101, doi: [10.1103/PhysRevLett.129.181101](https://doi.org/10.1103/PhysRevLett.129.181101)

Hunter, J. D. 2007, Computing in Science & Engineering, 9, 90, doi: [10.1109/MCSE.2007.55](https://doi.org/10.1109/MCSE.2007.55)

Jakobus, P., Müller, B., Heger, A., et al. 2022, Mon Not R Astron Soc, 516, 2554, doi: [10.1093/mnras/stac2352](https://doi.org/10.1093/mnras/stac2352)

Kluyver, T., et al. 2016, in *Positioning and Power in Academic Publishing: Players, Agents and Agendas*, ed. F. Loizides & B. Schmidt (IOS Press), 87–90

Kurkela, A., & Vuorinen, A. 2016, *Phys. Rev. Lett.*, 117, 042501, doi: [10.1103/PhysRevLett.117.042501](https://doi.org/10.1103/PhysRevLett.117.042501)

Kuroda, T., Fischer, T., Takiwaki, T., & Kotake, K. 2022, *ApJ*, 924, 38, doi: [10.3847/1538-4357/ac31a8](https://doi.org/10.3847/1538-4357/ac31a8)

Lonardoni, D., Tews, I., Gandolfi, S., & Carlson, J. 2020, *Phys. Rev. Research*, 2, 022033, doi: [10.1103/PhysRevResearch.2.022033](https://doi.org/10.1103/PhysRevResearch.2.022033)

Mogliacci, S., Andersen, J. O., Strickland, M., Su, N., & Vuorinen, A. 2013, *J. High Energ. Phys.*, 2013, 55, doi: [10.1007/JHEP12\(2013\)055](https://doi.org/10.1007/JHEP12(2013)055)

Montaña, G., Tolós, L., Hanuske, M., & Rezzolla, L. 2019, *Phys. Rev. D*, 99, 103009, doi: [10.1103/PhysRevD.99.103009](https://doi.org/10.1103/PhysRevD.99.103009)

Most, E. R., Motornenko, A., Steinheimer, J., et al. 2023, *Phys. Rev. D*, 107, 043034, doi: [10.1103/PhysRevD.107.043034](https://doi.org/10.1103/PhysRevD.107.043034)

Most, E. R., Papenfort, L. J., Dexheimer, V., et al. 2019, *Phys. Rev. Lett.*, 122, 061101, doi: [10.1103/PhysRevLett.122.061101](https://doi.org/10.1103/PhysRevLett.122.061101)

Nagata, K. 2022, *Progress in Particle and Nuclear Physics*, 127, 103991, doi: [10.1016/j.ppnp.2022.103991](https://doi.org/10.1016/j.ppnp.2022.103991)

Naseri, M., Bozzola, G., & Paschalidis, V. 2024, *Phys. Rev. D*, 110, 044037, doi: [10.1103/PhysRevD.110.044037](https://doi.org/10.1103/PhysRevD.110.044037)

O'Connor, E., & Ott, C. D. 2010, *Class. Quantum Grav.*, 27, 114103, doi: [10.1088/0264-9381/27/11/114103](https://doi.org/10.1088/0264-9381/27/11/114103)

Oertel, M., Hempel, M., Klähn, T., & Typel, S. 2017, *Rev. Mod. Phys.*, 89, 015007, doi: [10.1103/RevModPhys.89.015007](https://doi.org/10.1103/RevModPhys.89.015007)

Paschalidis, V., Yagi, K., Alvarez-Castillo, D., Blaschke, D. B., & Sedrakian, A. 2018, *Phys. Rev. D*, 97, 084038, doi: [10.1103/PhysRevD.97.084038](https://doi.org/10.1103/PhysRevD.97.084038)

Pierre Jacques, T., Cupp, S., Werneck, L. R., et al. 2025, *Phys. Rev. D*, 112, 084044, doi: [10.1103/PhysRevD.112.084044](https://doi.org/10.1103/PhysRevD.112.084044)

Prakash, A., Radice, D., Logoteta, D., et al. 2021, *Phys. Rev. D*, 104, 083029, doi: [10.1103/PhysRevD.104.083029](https://doi.org/10.1103/PhysRevD.104.083029)

Radice, D., Rezzolla, L., & Galeazzi, F. 2014, *Mon. Not. Roy. Astron. Soc.*, 437, L46, doi: [10.1093/mnrasl/slt137](https://doi.org/10.1093/mnrasl/slt137)

Radice, D., Rezzolla, L., & Galeazzi, F. 2014, *Class. Quantum Grav.*, 31, 075012, doi: [10.1088/0264-9381/31/7/075012](https://doi.org/10.1088/0264-9381/31/7/075012)

Rezzolla, L., Pizzochero, P., Jones, D. I., Rea, N., & Vidaña, I., eds. 2018, *Astrophysics and Space Science Library*, Vol. 457, *The Physics and Astrophysics of Neutron Stars* (Springer), doi: [10.1007/978-3-319-97616-7](https://doi.org/10.1007/978-3-319-97616-7)

Rezzolla, L., & Zanotti, O. 2013, *Relativistic Hydrodynamics* (Oxford University Press), doi: [10.1093/acprof:oso/9780198528906.001.0001](https://doi.org/10.1093/acprof:oso/9780198528906.001.0001)

Sagert, I., Fischer, T., Hempel, M., et al. 2009, *Phys. Rev. Lett.*, 102, 081101, doi: [10.1103/PhysRevLett.102.081101](https://doi.org/10.1103/PhysRevLett.102.081101)

Shashank, S., Nouri, F. H., & Gupta, A. 2023, *New Astronomy*, 104, 102067, doi: [10.1016/j.newast.2023.102067](https://doi.org/10.1016/j.newast.2023.102067)

Takami, K., Rezzolla, L., & Yoshida, S. 2011, *Mon. Not. R. Astron. Soc.*, 416, L1, doi: [10.1111/j.1745-3933.2011.01085.x](https://doi.org/10.1111/j.1745-3933.2011.01085.x)

Timmes, F. X., Woosley, S. E., & Weaver, T. A. 1996, *Astrophys. J.*, 457, 834, doi: [10.1086/176778](https://doi.org/10.1086/176778)

Ujevic, M., Gieg, H., Schianchi, F., et al. 2023, *Phys. Rev. D*, 107, 024025, doi: [10.1103/PhysRevD.107.024025](https://doi.org/10.1103/PhysRevD.107.024025)

Verma, A., Saha, A. K., Malik, T., & Mallick, R. 2025, *ApJ*, 988, 258, doi: [10.3847/1538-4357/ade9a2](https://doi.org/10.3847/1538-4357/ade9a2)

Weih, L. R., Hanuske, M., & Rezzolla, L. 2020, *Phys. Rev. Lett.*, 124, 171103, doi: [10.1103/PhysRevLett.124.171103](https://doi.org/10.1103/PhysRevLett.124.171103)

Zha, S., O'Connor, E. P., & Da Silva Schneider, A. 2021, *ApJ*, 911, 74, doi: [10.3847/1538-4357/abec4c](https://doi.org/10.3847/1538-4357/abec4c)